August, 1979] BULLETIN OF THE CHEMICAL SOCIETY OF JAPAN, VOL. 52 (8), 2281—2286 (1979) 2281

Curve Fitting Methods Applied to the Elucidation of Asymmetric Gas-Liquid Chromatographic Peaks

Koji Takeuchi and Tomihito Kambara*
Department of Chemistry, Faculty of Science, Hokkaido University, Sapporo 060

(Received September 8, 1978)

It was shown that the shape of gas-liquid chromatographic peak is expressed by the Gaussian distribution multiplied by a higher order algebraic equation of time. Application of the curve fitting methods, *i.e.*, the Newton's divided-difference formula and the orthogonal polynomials method, could well clear up the experimentally observed gas-liquid chromatograms of trailing and leading types, respectively. The asymmetric shapes of gas-liquid chromatographic peaks are attributed to the slowness of vaporization or dissolution in the partition process.

Although one observes in general the trailing type peaks in gas-solid adsorption chromatography, in gas-liquid partition chromatography the peaks of trailing and leading shapes[1–3] are observed at higher and lower column temperatures, respectively.

As to the asymmetric shapes of gas chromatographic peaks, there has been given only a qualitative explanation that the partition isotherm of a solute component between the mobile and stationary phases is nonlinear, as described in the several monographs.[4–6] A mathematical model for nonlinear partition based on the numerical solution by means of computer was proposed.[7] The theory by Schmauch[8] explains only the leading type peak, and on the contrary the papers by the Littlewood school[9,10] and others[11,12] deal with only the trailing peak expressed as the convolution of exponential decay constant. The derivative method for gas chromatograph developed by Saitoh *et al.*[2,13–17] is not only very useful in trace analysis but also gives important knowledges about the asymmetric shapes.

It is pointed out that the rate of vaporization is slow at lower temperature and on the other hand the rate of dissolution into stationary phase becomes too small at higher temperature, hence the partition equilibrium does hold no more. In this case a new theory dealing with the kinetically irreversible partition process between both phases is required.

As reported in our previous paper[18] the asymmetric gas-liquid chromatographic peaks are expressed by the series consisting of the Gaussian distribution G and its derivatives. In this paper the familiar curve fitting methods are applied to the mathematical analysis of the experimentally observed gas-liquid chromatograms of leading and trailing shapes.

Theoretical

The system of differential equations given by Kambara and Ohzeki[19] is as follows:

$$F\frac{\partial C}{\partial t} = -F\frac{\partial}{\partial x}\left(-\frac{D^*}{P}\frac{\partial C}{\partial x}+uC\right) + \alpha(K^{-1}C_s-C) \qquad (1)$$

$$F_s\frac{\partial C_s}{\partial t} = -\alpha(K^{-1}C_s-C) \qquad (2)$$

Equations 1 and 2 represent the concentration changes of the injected solute with time in the mobile and stationary phases, respectively. The meanings of symbols are summarized in Table 1. When the column temperature is lower than the optimum temperature, the rate of vaporization $\alpha K^{-1}C_s$ may be much smaller than that of dissolution αC. On the contrary, αC may be much smaller compared with $\alpha K^{-1}C_s$ at higher temperature. It is thus considered that the partition equilibrium would not hold at the column temperature much higher or lower than the optimum one.

The approximate solution of Eqs. 1 and 2 has been already presented as[19]

$$C(l,t) = \frac{p_o C_0 t_0}{p_i\sqrt{2\pi}\sigma}\exp\left(-\frac{(t-t_R)^2}{2\sigma^2}\right). \qquad (3)$$

On the basis of this expression the dependences of HETP on the flow rate of carrier gas,[20] on the column temperature[21] and on the column length[22] are elegantly clarified. For the convenience of the following treatment, one writes

$$\frac{p_o C_0 t_0}{p_i} = A, \qquad (4)$$

$$t - t_R = \xi, \qquad (5)$$

$$G(\xi) = \frac{1}{\sqrt{2\pi}\sigma}\exp\left(-\frac{\xi^2}{2\sigma^2}\right). \qquad (6)$$

Therefore, Eq. 3 can be written as the product of peak area A and the normal or Gaussian distribution $G(\xi)$:

$$C(l,\xi) = AG(\xi) \qquad (7)$$

At the appropriate temperature, both the rates of dissolution and vaporization being great, the term in the left-hand side of Eq. 2 is negligibly small compared with the two terms in the right-hand side. Then, one has

$$C_s(l,\xi) = KC = KAG(\xi). \qquad (8)$$

Namely, the equilibrium holds at every position in the column. At higher or lower temperature, the concentrations in both phases are no more equilibrated. In this case one should treat the problem kinetically. As derived in our previous paper[18] the outlet concentration is shown by

$$C(l,\xi) = A(G \pm zG^{(1)} + z^2G^{(2)} \pm z^3G^{(3)} + z^4G^{(4)} \pm z^5G^{(5)} + \cdots), \qquad (9)$$

where plus sign holds for trailing peak and minus sign for leading peak, respectively.

Furthermore, Eq. 9 can be rewritten in the alternative form. Derivatives of Gaussian distribution $G^{(n)}$ are calculated as

$$G^{(1)} = -\frac{\xi}{\sigma^2}G(\xi) \qquad (10)$$

Table 1. List of symbols

Symbol	Meaning	Units
A	peak area	mol s cm^{-3}
a_i	coefficient in Eq. 12	s^{-i}
b	z/σ	dimensionless
C	solute concentration in mobile phase	mol cm^{-3}
$C(l, \xi)$	outlet concentration in mobile phase, dependent on ξ	mol cm^{-3}
C_s	solute concentration in stationary phase	mol cm^{-3}
$C_s(l, \xi)$	outlet concentration in stationary phase, dependent on ξ	mol cm^{-3}
C_0	initial solute concentration injected	mol cm^{-3}
D^*	diffusion constant at unit pressure	cm^2 s^{-1} atm
F	volume fraction occupied by mobile phase	dimensionless
F_s	volume fraction occupied by stationary phase	dimensionless
$G(\xi)$	Gaussian distribution described by Eq. 6	s^{-1}
$G^{(n)}$	n-th derivative of $G(\xi)$	s$^{-(n+1)}$
h	peak height	mol cm^{-3}
K	partition coefficient (C_s/C at equilibrium)	dimensionless
l	column length	cm
p	pressure of carrier gas dependent on x	atm
p_i	pressure of carrier gas at column inlet	atm
p_o	pressure of carrier gas at column outlet	atm
R	skew ratio	dimensionless
t	time elapsed after solute fed	s
t_R	retention time of solute component	s
t_0	duration of concentration pulse injected	s
u	linear gas velocity dependent on x	cm s^{-1}
x	distance from inlet along the column	cm
y	a function expressed by $C(l, \xi)/AG(\xi)$	dimensionless
z	F_sK/α	s
α	rate constant of dissolution of solute	s^{-1}
σ^2	peak variance	s^2
ξ	time measured from retention time defined by Eq. 5	s

$$G^{(2)} = \frac{1}{\sigma^2}\left(\frac{\xi}{\sigma^2}-1\right)G(\xi). \tag{11}$$

Insertion of these derivatives into Eq. 9 gives the following Eq. 12 in which the elution profile $C(l, \xi)$ is a product of $AG(\xi)$ and a high-order algebraic equation of ξ.

$$\begin{aligned} C(l, \xi) = AG(\xi)(a_0+a_1\xi+a_2\xi^2+a_3\xi^3 \\ +a_4\xi^4+a_5\xi^5+\cdots) \end{aligned} \tag{12}$$

The coefficient a_i (i=0, 1, 2, $\cdots$) is given by

$$\begin{aligned} a_0 &= 1 - b^2 + 3b^4 - \cdots \\ a_1 &= \pm\sigma^{-1}(b-3b^3+15b^5-\cdots) \\ a_2 &= \sigma^{-2}(b^2-6b^4+45b^6-\cdots) \\ a_3 &= \pm\sigma^{-3}(b^3-10b^5+105b^7-\cdots) \\ a_4 &= \sigma^{-4}(b^4-15b^6+210b^8-\cdots) \\ a_5 &= \pm\sigma^{-5}(b^5-21b^7+378b^9-\cdots) \end{aligned} \tag{13}$$

where

$$b = \frac{z}{\sigma} \tag{14}$$

Thus, a theoretical expression for the asymmetric elution profiles in partition chromatography is shown by Eq. 9 or 12, which is reduced to Eq. 3 when z tends to zero.

According to Eq. 12, $C(l, \xi)$ divided by $AG(\xi)$ is defined as

$$\begin{aligned} y = \frac{C(l, \xi)}{AG(\xi)} = a_0 + a_1\xi + a_2\xi^2 + a_3\xi^3 \\ + a_4\xi^4 + a_5\xi^5 + \cdots \end{aligned} \tag{15}$$

Experimental

Reagents and Apparatus. Helium was used as the carrier gas. Benzene and diethyl ether (Wako Pure Chemicals Co.) were used as solute and diluent, respectively. A Hitachi gas chromatograph, Model 063, with a flame ionization detector was employed. The output current of FID was amplified and then recorded with a Hitachi 056 recorder. The packing of 25% dinonyl phthalate on 60/80 mesh Shimalite supplied by Shimadzu Seisakusho Ltd. was packed into a stainless steel column of 4 mm i.d. and 1 m in length. A soap-film flowmeter was used for the measurement of flow rate.

The column temperature was varied in the range of 45.7—93.0 °C and maintained within ±0.1 °C of the set temperature. The temperatures of injection port and detector were fixed at 105 °C. Carrier gas flow rate was adjusted to 30.0±0.3 ml min^{-1}.

The solute amount smaller than 0.8 μl was confirmed to have no effect on the number of theoretical plates for benzene. Therefore, a 5-μl portion of benzene diluted 10-fold with diethyl ether was injected. The gas chromatograms are reproduced in Fig. 1.

Estimation of t_R and σ. The apparent retention time as measured at the peak maximum depends slightly on the solute amount fed when the column temperature deviates from the optimum one. The chromatograms with varying amounts of

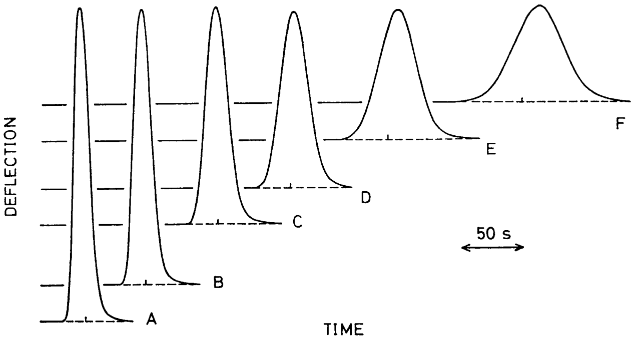

Fig. 1. Gas chromatograms of benzene at various temperatures. Sample size injected was 0.5 μl and detected by FID. Each peak was corrected for the temperature dependence of detector sensitivity to have the same peak area. Column temperature: A 93.0, B 83.3, C 74.1, D 64.8, E 55.0, F 45.7 °C. The mark on the base line indicates the corrected retention time. The other data are shown in Table 5.

benzene smaller than 0.5 μl were accurately superimposed on the one with 0.5 μl so as to give the true retention time. Retention time was determined by extrapolating the solute amount to zero, *i.e.*, at the point on which the line connecting the maxima of the peaks intersects the base line, as Fig. 2 shows.

The standard deviation σ, namely, the square root of the peak variance needs to be estimated. It was presumed that the quantity 2σ is given by the peak width at the peak height of $e^{-1/2}\cdot h$, where h is the maximum peak height. Peak area A was calculated by the so-called trapezoidal rule with the known $C(l, \xi)$ values at equi-spaced points. Skew ratio R is defined as the ratio of the slopes of tangents at the inflection points on both sides of the peak,[24] and calculated for each chromatogram as a measure of asymmetry.

Curve Fitting Methods. The mathematical expression for the experimentally observed y-function shown by Eq. 15 was determined by means of the familiar curve fitting methods. One is the Newton's divided-difference formula[25] and the other is the orthogonal polynomials.[25,26] The former is one of the interpolation formula which is advantageous in treating with a curve of the complicated form such as the results observed at higher temperatures (curves d and d′ in Fig. 2). The latter is the most general method of curvilinear regression by the method of least squares and suitable for the simple and monotone function as seen in the case obtained at lower temperatures (curves c and c′ in Fig. 2). Another advantage of the orthogonal polynomials is that one can easily decide what order of polynomials should be statistically significant when the analysis of variance table is constructed. The algebraic equations determined are plotted and this operation is repeated until the satisfactory fitting is confirmed.

Results and Discussion

The theoretical elution profiles were calculated with the derivative series including the fifth order derivative shown by Eq. 9, as reported before. When the value z was smaller than $0.45\,\sigma$, Eq. 9 was found to fit well. A symmetric Gaussian peak is obtained when $z=0$ and the distortion of peak becomes more remarkable with increasing value of z. Skew ratio R was evaluated as 1.06 (leading), 0.94 (trailing) with $z=0.40\,\sigma$; 1.68 (leading), 0.60 (trailing) with $z=0.45\,\sigma$. With z-value greater than $0.45\,\sigma$, Eq. 9 represents an inadequate curve, the concentration $C(l, \xi)$ showing negative values at the feet of the peak.

Thus Eq. 9 was confirmed to express well the asymmetric curves of both leading and trailing types. Furthermore, another verification of Eq. 9 with experimental chromatograms was attempted. Chromatograms with varying solute amounts of 0.1—0.5 μl were carefully superimposed on a chart. Figure 2 shows the typical leading and trailing chromatograms of benzene and the mathematical analysis of y-function.

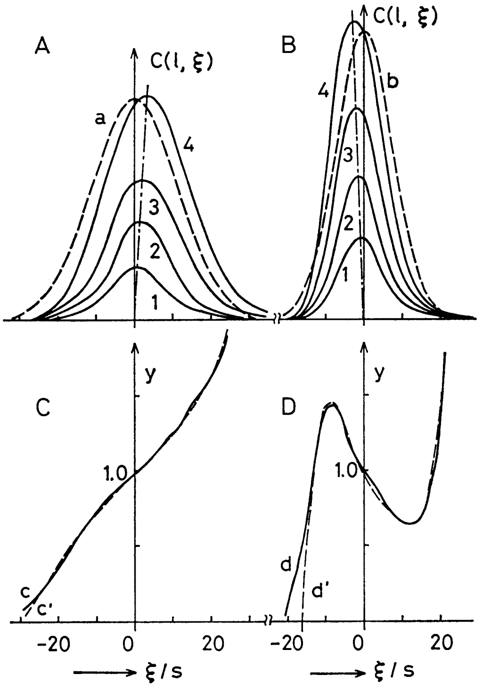

Fig. 2. Comparison of the experimentally recorded leading (curves A, 64.8 °C) and trailing (curves B, 83.3 °C) gas chromatograms of benzene (solid line) with the Gaussian peaks of the same σ-values (dashed line, curves a and b). The amount of benzene injected: 1 0.1, 2 0.2, 3 0.3, 4 0.5 μl. Curves C and D show the y-functions given by Eq. 15. Curves c and d (solid line): experimental value; curves c′ and d′ (dashed line): calculated value.

With increasing solute amount injected, the apparent rentention time of the peak maximum becomes longer in the case of leading peak, and on the contrary, it becomes shorter in the case of trailing peak (A and B in Fig. 2). The values of t_R, σ, and A were evaluated and the curves $AG(\xi)$ (dashed line, a and b in Fig. 2), which might be considered as a well-equilibrated elution profile of Gaussian type, were plotted for reference. The ratio of $C(l, \xi)$ to $AG(\xi)$ defined as y in Eq. 15 was then evaluated from experimental data (solid line, curves c and d in Fig. 2). The theoretical equations for these experimentally obtained y-functions were determined by the curve fitting methods (dashed line, curves c′ and d′). In the case of data at 83.3 °C, the Newton's divided-difference formula was applied as shown in Table 2. Several characteristic points including maximum, mini-

TABLE 2. CURVE FITTING METHOD. NEWTON'S DIVIDED-DIFFERENCE FORMULA[a)]

ξ/s	y	Divided difference[b)]				
−12	1.2153					
		0.05308				
−8	1.4276		−0.01119			
		−0.0588		$6.936 \cdot 10^{-4}$		
−2	1.0748		0.001296		$-2.83 \cdot 10^{-5}$	
		−0.0407		$1.369 \cdot 10^{-5}$		$1.245 \cdot 10^{-6}$
6	0.7496		0.001570		$6.534 \cdot 10^{-6}$	
		−0.0187		$1.705 \cdot 10^{-4}$		
12	0.6367		0.004639			
		0.02773				
16	0.7485					

a) Data of 83.3 °C were analysed. b) The y-function is expressed as follows. $y=1.2153+0.05308\ (\xi+12)$ $-0.01119\ (\xi+12)\ (\xi+8)\ +6.936 \cdot 10^{-4}\ (\xi+12)\ (\xi+8)\ (\xi+2)\ -2.833 \cdot 10^{-5}\ (\xi+12)\ (\xi+8)\ (\xi+2)\ (\xi-6)$ $+1.245 \cdot 10^{-6}\ (\xi+12)\ (\xi+8)\ (\xi+2)\ (\xi-6)\ (\xi-12)$ $=0.9612\ -0.0508\,\xi\ +0.003121\,\xi^2\ +6.243 \cdot 10^{-6}\,\xi^3\ -2.3347 \cdot 10^{-5}\,\xi^4\ +1.245 \cdot 10^{-6}\,\xi^5$.

TABLE 3. CURVE FITTING METHOD. ORTHOGONAL POLYNOMIALS AND THE CALCULATION TABLE[a)]

		Polynomials from zero to fifth order[b)]							
		P_0	P_1	P_2	P_3	P_4	P_5	y	y^2
ξ	−26	1	−13	325	−130	2990	−16445	0.1488	0.0221
	−24	1	−12	250	−70	690	2530	0.2196	0.0483
	−22	1	−11	181	−22	−782	10879	0.2877	0.0828
	0	1	0	−182	0	1638	0	0.9748	0.9502
	26	1	13	325	130	2990	16445	2.0727	4.2961
a_{ii}		27	1638	712530	101790	56448210	2032135560	$\sum y^2$	34.0625
λ_i		1	1	3	1/6	7/12	21/40		
β_i		1.0016	0.064735	$5.244 \cdot 10^{-4}$	$1.4291 \cdot 10^{-4}$	$7.1918 \cdot 10^{-6}$	$4.47 \cdot 10^{-8}$		

		$P_0 y$	$P_1 y$	$P_2 y$	$P_3 y$	$P_4 y$	$P_5 y$
ξ	−26		−1.9344	48.36	−19.34	444.91	−2447.0
	−24	equal to y	−2.6352	54.90	−15.37	151.52	555.6
	−22		−3.1647	52.07	−6.33	−224.98	3129.9
	0		0	−177.41	0	1596.72	0
	26		26.9451	673.63	269.45	6197.37	34085.6
$\sum P_i y$		27.0442	106.0365	124.5588	87.2792	695.9422	173.0

a) Data of 64.8 °C, sample number $n=27$, sample space $h=2$. b) Values of orthogonal polynomials (P_i), its sum of squares (a_{ii}) and coefficient (λ_i) are quoted from Ref. 26. $\beta_i=\frac{\lambda_i \sum P_i y}{a_{ii}}$, $P_0(d)=1$, $P_1(d)=d$, $P_2(d)=d^2-\frac{1}{12}(n^2-1)$, $P_3(d)=d^3-\frac{1}{20}(3n^2-7)d$, $P_4(d)=d^4-(3n^2-13)d^2+\frac{3}{560}(n^2-1)(n^2-9)$, $P_5(d)=d^5-\frac{5}{18}(n^2-7)d^3+\frac{1}{1008}(15n^2-230n^2+407)d$ where $d=\frac{\xi-\bar{\xi}}{h}$. The regression equation is given by $y=\beta_0 P_0(d)+\beta_1 P_1(d)+\beta_2 P_2(d)+\beta_3 P_3(d)+\cdots$ Thus, in this case, the following regression equation is obtained. $y=0.9900+0.02458\xi-1.481 \cdot 10^{-4}\xi^2+1.786 \cdot 10^{-5}\xi^3+4.495 \cdot 10^{-7}\xi^4$.

mum and inflection points are picked up and the difference between the adjacent y values is divided by the difference in ξ. Upon repeating this calculation, the interpolation equation is obtained as shown in Table 2.

In the case of data at 64.8 °C, the method of orthogonal polynomials was applied and the result is given in Table 3. In the calculation table the values of orthogonal polynomials P_i are cited, and the values of y, y^2 and $P_i y$ are evaluated from the experimental data. Then the product of the coefficient λ_i and $\sum P_i y$ is divided by a_{ii} to give β_i which is the coefficient of the orthogonal polynomial of i-th order. The orthogonal polynomials can be added to an arbitrary higher order until the satisfactory fitting is obtained. The analysis of variance table given in Table 4 shows that for the data of 64.8 °C the fifth order polynomial is not significant since the sum of squares contributed by the fifth order term is smaller than the residual. Therefore, the use of polynomials until fourth order is sufficient in this case.

An excellent agreement between the experimental

Table 4. Analysis of variance in orthogonal polynomials

Source of variance	Sum of squares[a)]	
	55.0 °C	64.8 °C
1st order	13.280504	6.864310
2nd	1.174419	0.021774
3rd	0.083573	0.074837
4th	0.001454	0.008580
5th	0.000634	0.000015
Residual	0.005212	0.004542
Total	14.545796[b)]	6.974058

a) Calculated by $\frac{(\sum P_i y)^2}{a_{ii}}$. b) Calculated by $\sum y^2 - \frac{(\sum y)^2}{a_{00}}$.

values and the calculated y-function was seen in Fig. 2. This treatment shows that curves c and d were fourth and fifth order algebraic equations of ξ, respectively. The deviations in the feet of a peak where the absolute value of ξ is large, may be caused by the measuring error.

Thus, the actual chromatograms of leading and trailing types were found to be reasonably expressed by Eq. 12. Consequently, the present theoretical treatment can well clear up the asymmetric peak shapes. The results successfully obtained by the curve fitting methods for chromatograms at various temperatures were tabulated in Table 5.

The retention time as well as the standard deviation decreases with increasing temperature. Although the skew ratio R also decreases with increasing temperature, it lies at about 0.87 at the optimum temperature of 73.7 °C, deviating a little from unity. As for the coefficients in Eq. 12, the first term a_0 shows its maximum value near the optimum temperature, since the degree of symmetry is mainly governed by a_0.

Development of the Kinetic Theory. Proposal of the present theory is quite similar to the development of the polarographic theory. In 1935 Heyrovsky and Ilkovic postulated the dynamic equilibrium of oxidant and reductant concentrations at the surface of dropping mercury electrode depending on the potential. Thus they succeeded in elucidating the reversible wave, as described in several monographs.[27–29] Later in 1950's several kinetic theories were proposed dealing with the irreversible reduction in which the concentrations of oxidant and reductant are not equilibrated at the electrode surface.

Thanks are due to Dr. Kunio Ohzeki for his kind discussions.

References

1) T. Kambara and H. Kodama, *J. Chromatogr.*, **17**, 66 (1965).

2) T. Kambara, and K. Saitoh, *J. Chromatogr.*, **35**, 318 (1968).

3) K. Saitoh and T. Kambara, *Bunseki Kagaku*, **20**, 1375 (1971).

4) A. B. Littlewood, "Gas Chromatography," Academic Press, London (1962), p. 12.

5) H. Purnell, "Gas Chromatography," John Wiley and Sons, New York (1962), p. 82.

6) A. I. M. Keulemans, "Gas Chromatography," 2nd ed, ed by C. G. Verver, Reinhold, New York (1959), Chap. 4.

7) J. E. Funk and G. Houghton, *Nature*, **188**, 389 (1960).

8) L. J. Schmauch, *Anal. Chem.*, **31**, 225 (1959).

9) A. H. Anderson, T. C. Gibb, and A. B. Littlewood, *Anal. Chem.*, **42**, 434 (1970).

10) A. H. Anderson, T. C. Gibb, and A. B. Littlewood, *J. Chromatogr. Sci.*, **8**, 640 (1970).

11) W. W. Yau, *Anal. Chem.*, **49**, 395 (1977).

12) R. E. Pauls and L. B. Rogers, *Anal. Chem.*, **49**, 625 (1977).

13) T. Kambara, K. Saitoh, and K. Ohzeki, *Bunseki Kagaku*, **15**, 517 (1966).

14) T. Kambara, K. Saitoh, and K. Ohzeki, *Anal. Chem.*, **39**, 409 (1967).

15) T. Kambara, K. Saitoh, and K. Ohzeki, *Bunseki Kagaku*, **16**, 721 (1967).

16) T. Kambara, S. Katada, and K. Saitoh, *Bunseki Kagaku*, **18**, 1225 (1969).

17) K. Saitoh and T. Kambara, *Kagaku No Ryoiki*, **23**, 11 (1969).

18) K. Takeuchi and T. Kambara, *Chem. Lett.*, **1978**, 1081.

19) T. Kambara and K. Ohzeki, *J. Chromatogr.*, **21**, 383 (1966).

20) T. Kambara, K. Ohzeki, and K. Saitoh, *J. Chromatogr.*, **27**, 33 (1967).

21) T. Kambara, K. Hata, and K. Ohzeki, *J. Chromatogr.*, **37**, 304 (1968).

22) K. Ohzeki, T. Kambara, and K. Kodama, *J. Chromatogr.*, **121**, 199 (1976).

23) Ref. 4, p. 166, Eqs. 5.55 and 5.56.

Table 5. Characteristics of gas chromatograms observed with varying temperatures[a)]

Temp/°C	t_R/s	σ/s	R	Method[b)]	Coefficients in Eq. 12 determined					
					a_0	10^2a_1	10^3a_2	10^5a_3	10^5a_4	10^6a_5
45.7	591.9	20.0	1.084	o.p.	0.7745	2.624	0.522	0.572	0	0
55.0	430.8	14.85	1.067	o.p.	0.8587	3.114	0.582	0.815	0	0
64.8	305.7	11.1	0.940	o.p.	0.9900	2.458	−0.148	1.786	0.045	0
73.3	237.2	8.9	0.923	o.p.	1.0645	1.776	−1.306	3.467	0.199	0
74.1	234.0	9.1	0.812	N	1.0755	−1.411	−0.988	7.622	0.059	0
83.3	183.2	7.25	0.698	N	0.9612	−5.079	3.121	0.624	−2.335	1.245
93.0	145.6	6.35	0.638	N	0.9078	−7.090	4.260	−4.703	−2.193	1.537

a) 25% DNP on 60/80 mesh Shimalite in 4 mm i.d., 1 m stainless column; carrier gas He 30 ml min^{-1}; detector FID. b) o.p. = orthogonal polynomials, N = Newton's divided-difference formula.

24) A. J. B. Cruickshank and D. H. Everett, *J. Chromatogr.*, **11**, 289 (1963).

25) C. R. Wylie, Jr., "Advanced Engineering Mathematics," McGraw-Hill, New York (1966), Chap. 4.

26) "Statistical Tables and Formulas with Computer Applications. JSA-1972," ed by Z. Yamauti, Japan Standards Association, Tokyo (1972), pp. 407—417.

27) P. Delahay, "New Instrumental Methods in Electrochemistry," Interscience Publishers, Inc., New York (1954), Chaps. 3 and 4.

28) J. Heyrovsky and J. Kuta, "Principles of Polarography," Academic Press, New York (1965), Chaps. 9 and 13.

29) G. Charlot, J. Badoz-Lambling and B. Trémillon, "Les Réactions Electrochimiques. Méthodes Electrochimiques d'Analyse," Masson, Paris (1959), Chaps. 3 and 4. English translation: "Electrochemical Reactions. The Electrochemical Methods of Analysis," Elsevier, Amsterdam (1962).